



Behavior of strain at a thin Ge pile-up layer formed by dry oxidation of a $\text{Si}_{0.7}\text{Ge}_{0.3}$ film

B.-G. Min ^{a,1}, J.-H. Yoo ^a, H.-C. Sohn ^a, D.-H. Ko ^{a,*}, M.-H. Cho ^b, K.-B. Chung ^c, T.-W. Lee ^d

^a Department of Materials Science and Engineering, Yonsei University, 134 Shinchon, Seodaemun, Seoul 120-749, Korea

^b Institute of Physics and Applied Physics, Yonsei University, 134 Shinchon, Seodaemun, Seoul 120-749, Korea

^c Department of Physics, North Carolina State University, Raleigh, NC 27695-8202 USA

^d Jusung Engineering Co., Ltd., 49, Neungpyeong-ri, Opo-eup, Gwangju-Si, Kyunggi-do, Korea, 464-892, Korea

ARTICLE INFO

Article history:

Received 21 February 2009

Received in revised form 30 June 2009

Accepted 19 July 2009

Available online 26 July 2009

Keywords:

$\text{Si}_{1-x}\text{Ge}_x$

Oxidation

Ge pile-up layer

Relaxation

Medium energy ion scattering

Strain

ABSTRACT

The change of strain in $\text{Si}_{0.7}\text{Ge}_{0.3}$ films was investigated with medium energy ion scattering (MEIS). Si was removed in the films by selective oxidation at 800 °C, resulting in the formation of a Ge pile-up layer on the surface. The relaxation and the thickness of the pile-up layer were closely related to the oxidation time. MEIS data demonstrated that relaxation of the Ge layer in the depth direction occurred partially, and that the rates of relaxation decreased with depth. In addition, the rate of relaxation increased with the oxidation time. Lastly, the relaxation of the Ge layer affected the strain of the remaining $\text{Si}_{0.7}\text{Ge}_{0.3}$ substrate.

© 2009 Elsevier B.V. All rights reserved.

1. Introduction

Strained Si channel structures have been used to create high performance ultralarge-scale integration devices because high mobility can be achieved when using such channels [1–7]. Many materials and various structures have been used to produce strained Si channels; among the materials that have attracted considerable attention is $\text{Si}_{1-x}\text{Ge}_x$, which is a candidate because the strain of $\text{Si}_{1-x}\text{Ge}_x$ is easily controlled by varying the concentration of Ge in the film. However, implementation of this process is difficult for conventional complementary metal-oxide-semiconductor processes due to the long process time that is required to grow thick relaxed $\text{Si}_{1-x}\text{Ge}_x$. Moreover, this process cannot be easily applied to the formation of particular structures such as strained Si/relaxed $\text{Si}_{1-x}\text{Ge}_x/\text{SiO}_2/\text{Si}$ (SGOI) and strained $\text{Si}/\text{SiO}_2/\text{Si}$ (SSOI). Previously, it has been reported that relaxed $\text{Si}_{1-x}\text{Ge}_x$ can be formed by using the characteristics of selective oxidation of $\text{Si}_{1-x}\text{Ge}_x$ [8,9]; this technique decreases the required thickness of relaxed $\text{Si}_{1-x}\text{Ge}_x$ in SGOI structure and removes the wafer bonding and the wafer polishing process to form the SGOI structure. During the oxidation of $\text{Si}_{1-x}\text{Ge}_x$, only Si is selectively oxidized while Ge, which does not participate in oxidation, is excluded from the oxide layer. Thus, a new Ge pile-up layer forms between the

oxide layer and the $\text{Si}_{1-x}\text{Ge}_x$ layer. This phenomenon has been reported in several other papers on the oxidation of $\text{Si}_{1-x}\text{Ge}_x$ [10–13]. However, because the thickness of the Ge pile-up layer formed by oxidation is too thin to be measured by normal strain measurement techniques, strain behavior has not been clearly studied during the selective oxidation of $\text{Si}_{1-x}\text{Ge}_x$. Therefore, in order to inspect the effect of oxidation for strain at early states of oxidation, we investigated the strain in Ge pile-up layers with a thickness of less than 15 nm using a medium energy ion scattering system.

2. Experimental details

50 nm-thick $\text{Si}_{1-x}\text{Ge}_x$ ($x=0.15$ and 0.3) films were epitaxially grown on HF-cleaned Si (100) wafers by ultra-high vacuum chemical vapor deposition (UHV-CVD, URECA 3000) at 550 °C. Si_2H_6 and GeH_4 were used as the Si and Ge sources, respectively. The base pressure in the UHV-CVD system was 1.3×10^{-6} Pa, and deposition of the $\text{Si}_{1-x}\text{Ge}_x$ films was performed at around 1.3×10^{-2} Pa. The presence of the Ge fraction was confirmed by Auger electron spectroscopy (AES) and Rutherford back-scattering analysis. After native oxides were removed by HF cleaning, samples were oxidized at 800 °C in a dry O_2 ambient using a vertical furnace. The microstructures of oxidized $\text{Si}_{0.7}\text{Ge}_{0.3}$ at 800 °C were observed by using transmission electron microscopy (TEM, JEM-3011). Electrons were generated using a field emission-type source and then accelerated up to 300 kV. The resolution of the TEM was

* Corresponding author. Fax: +82 2 365 5882.

E-mail address: dhko@yonsei.ac.kr (D.-H. Ko).

¹ Current address: Jusung Engineering Co., Kyunggi-do, Korea.

0.14 nm for the lattice image and 0.2 nm for the point image. After selective oxidation, the thermal oxide of SiO_2 was removed by HF cleaning to observe the separation of the Ge pile-up layer from the $\text{Si}_{0.7}\text{Ge}_{0.3}$ layer using medium energy ion scattering (MEIS). MEIS spectra were taken as functions of the scattering angle and the energy of the protons ejected from the samples. The angular resolution of the MEIS system was estimated to be 0.1° [14]. The primary beam energy of the proton was 100 keV and the current density of the incident beam was $5 \mu\text{Acm}^{-2}$. A single alignment condition was applied for the blocking dip measurement, in which the incident beam angle was displaced 2.5° from the (001) direction in the (011) plane, and the detected ion was in approximately the (111) direction.

3. Results and discussion

The microstructures of $\text{Si}_{0.7}\text{Ge}_{0.3}$ were oxidized at 800°C for either 30 or 120 min, and were investigated with high-resolution TEM measurements. As shown in Fig. 1, the strained $\text{Si}_{0.7}\text{Ge}_{0.3}$ and the Ge pile-up layer were clearly distinguished by their contrast. The germanium produced during the oxidation process accumulated in the $\text{Si}_{1-x}\text{Ge}_x$ layer just beneath the oxide by a snowplowing effect, because extracted Si from the $\text{Si}_{1-x}\text{Ge}_x$ reacted with oxygen, consistent with a previous report [15]. The thickness of the Ge pile-up layers increased from 3.6 nm to 8.2 nm with the increase in oxidation time. The Ge concentration in the Ge pile-up layers was greatest at the surface and gradually decreased towards the interface of the Ge pile-up layer and the remaining $\text{Si}_{0.7}\text{Ge}_{0.3}$ layer. The maximum Ge concentration at the top surface of the Ge pile-up layers in oxidized $\text{Si}_{0.7}\text{Ge}_{0.3}$ is 45% and 55% for 30 min and 120 min, respectively [15].

In order to inspect the strain relaxation during the oxidation of $\text{Si}_{1-x}\text{Ge}_x$, we observed the strain in the Ge pile-up layers and in the remaining $\text{Si}_{1-x}\text{Ge}_x$ layers using MEIS measurements. The shifts of Si (111) and Ge (111) blocking dips for as-deposited $\text{Si}_{0.7}\text{Ge}_{0.3}$ were plotted as a function of energy, as shown in Figs. 2–4. We derived the angle of (111) blocking dips for each energy of the MEIS spectra and the angles were fitted with a parabolic function in order to quantitatively evaluate the position of the Ge blocking dips.

The shift of Si and Ge from the Si (111) blocking dips for as-deposited $\text{Si}_{0.7}\text{Ge}_{0.3}$ became constant at all energies within the reported error range, as shown in Fig. 2. The energy of the detected ion corresponded to the depth from the surface in a sample, such that an ion scattered from a

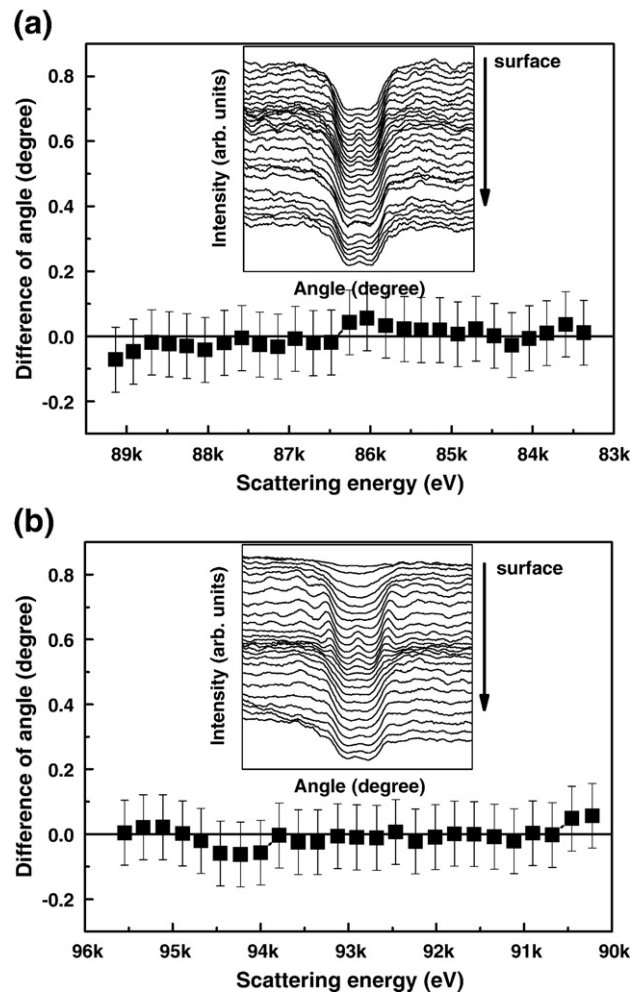


Fig. 2. Shift of the blocking dip positions of the (a) Si and (b) Ge peaks for as-deposited $\text{Si}_{0.7}\text{Ge}_{0.3}$.

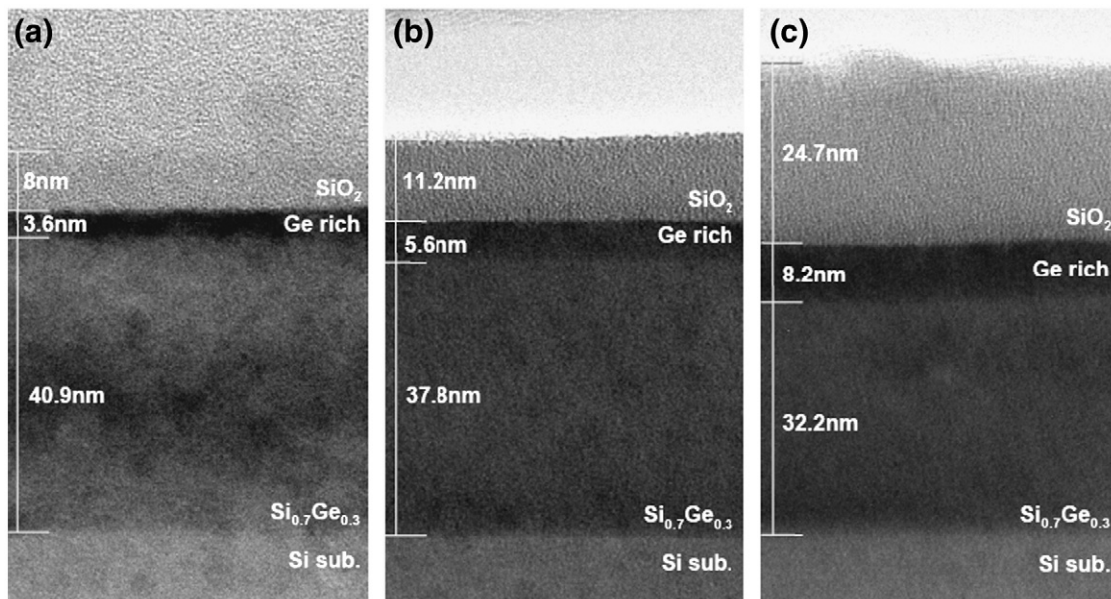


Fig. 1. TEM images of oxidized $\text{Si}_{0.7}\text{Ge}_{0.3}$ at 800°C after (a) 30 min, (b) 60 min, and (c) 120 min.

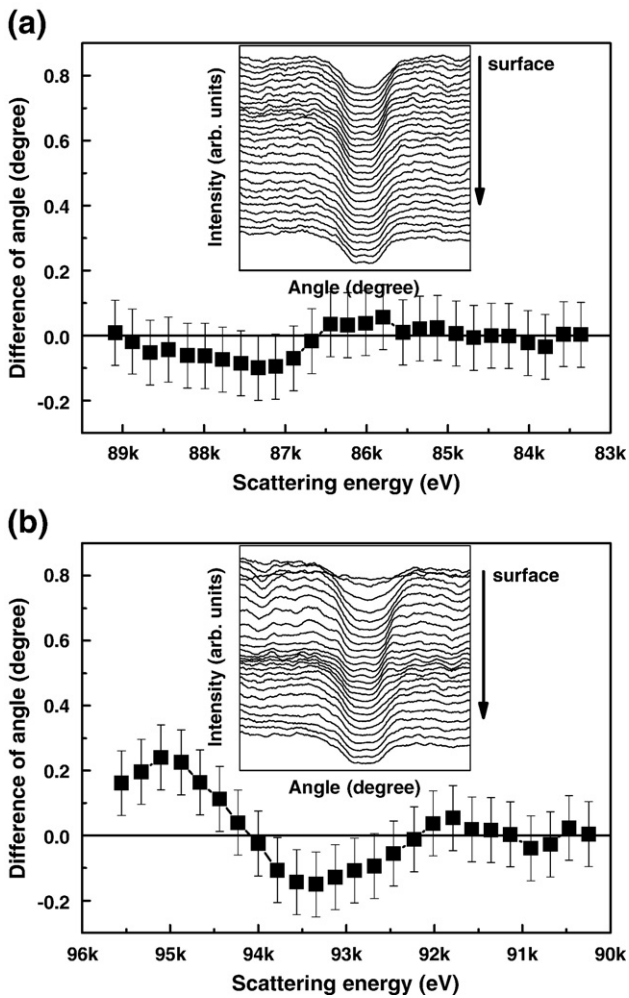


Fig. 3. Shift of the blocking dip positions of the (a) Si and (b) Ge peaks for $\text{Si}_{0.7}\text{Ge}_{0.3}$, which was oxidized for 30 min.

deeper layer in the sample had a lower energy than one scattered from the surface, because the energy loss during the ion scattering process increased with the depth of the scattered ion. Moreover, the shift of the blocking dip suggested that the position of the atom in the film blocking the scattered ion moved from the original position. Therefore, shift as a function of energy corresponded to the deformation of strain in as-deposited and oxidized $\text{Si}_{0.7}\text{Ge}_{0.3}$ at a particular depth. However, we did not observe any angular shift in Fig. 2, which indicated that the strain in as-deposited $\text{Si}_{0.7}\text{Ge}_{0.3}$ was constant with respect to depth direction. In a previous work [15], we used high-resolution x-ray diffraction measurements to show that as-deposited $\text{Si}_{0.7}\text{Ge}_{0.3}$ can be fully compressively strained. This is consistent with the MEIS data from the present study, because the maximum depth observed with the MEIS measurement was around 15 nm for Si in as-deposited 50 nm-thick $\text{Si}_{0.7}\text{Ge}_{0.3}$. Therefore, the strain in the as-deposited $\text{Si}_{0.7}\text{Ge}_{0.3}$ was fully compressive and uniform within the depths that were observable by MEIS measurements in our experiments.

Comparing the change in the blocking dip of the oxidized $\text{Si}_{0.7}\text{Ge}_{0.3}$ film in the depth direction with that of the as-deposited $\text{Si}_{0.7}\text{Ge}_{0.3}$, the shift of Ge (111) blocking dips of $\text{Si}_{0.7}\text{Ge}_{0.3}$ oxidized for 30 min can be clearly observed in Fig. 3. The shift of Ge (111) blocking dips of $\text{Si}_{0.7}\text{Ge}_{0.3}$ oxidized for 30 min was modulated in the depth direction such that the shift increased at 95.5 keV and decreased between 95.1 keV and 93.5 keV. After this decrease, the shifts of the Ge (111) blocking dips began to increase again until they became saturated at 92 keV. The shift of the Si (111) blocking dips of $\text{Si}_{0.7}\text{Ge}_{0.3}$ oxidized for 30 min was unclear

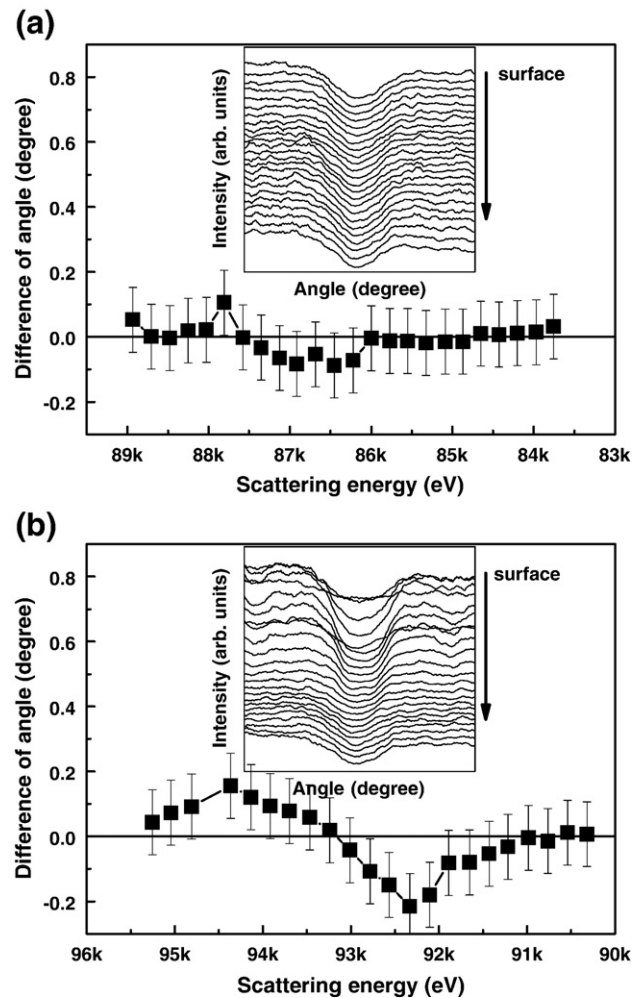


Fig. 4. Shift of the blocking dip positions of the (a) Si and (b) Ge peaks for $\text{Si}_{0.7}\text{Ge}_{0.3}$, which was oxidized for 120 min.

compared with the blocking data for Ge. The backscattered Si ions were more affected and absorbed by nuclear forces at the lattice point of the film because the energy of the backscattered Si ions was smaller than that of the Ge. Moreover, it is possible that the backscattered ions for Si at the surface of the Ge pile-up layer mixed with a small amount of Ge at a deeper depth. As shown in Fig. 3(a) and (b), the maximum energy of the backscattered ions for Si was similar to the minimum energy of Ge. Thus, if the backscattered ions for Si at the top surface and Ge in a deeper layer mixed, the shift of the Si (111) blocking dips by oxidation of $\text{Si}_{1-x}\text{Ge}_x$ would contain all of the information of these two layer types. Therefore, the incomparable modulus of Si was due to the absorption of backscattered ions for the small kinetic energy of Si and the intermixing of information for Si at the top surface and Ge in a deeper layer.

Fig. 4 shows that the shifts of the Ge (111) blocking dips occurred at a deeper depth in oxidized $\text{Si}_{0.7}\text{Ge}_{0.3}$ for 120 min, while the blocking dips of Si (111) also gave unclear results. The shifts of the Ge (111) blocking dips for 120 min exhibited a trend similar to that of 30 min, while the negative-shift region appeared at deeper depths (93–91 keV) as the concentration of Si decreased and the pile-up layer grew. The thickness of the positive-shift region increases with oxidation time as a result of the increase in the Ge pile-up layer, as shown in a previous report [15], as well in the present study (Fig. 1).

The change in the blocking dips, such as the depth position and shift angle, can give important information about the strain in the Ge pile-up layer and the remaining initial $\text{Si}_{0.7}\text{Ge}_{0.3}$. The Ge concentrations in the Ge pile-up layers were larger than in the remaining $\text{Si}_{0.7}\text{Ge}_{0.3}$ layers, and

gradually increased from the interface between the pile-up layer and the remaining $\text{Si}_{0.7}\text{Ge}_{0.3}$ layer to the surface of the pile-up layer. Moreover, the difference in the shift direction between the upper pile-up layer and deeper region indicated that different strains were generated in the film surface and in deeper regions, depending on the oxidation condition. According to a previous work [16,17], the horizontal (a_{SiGe}^{\perp}) and vertical ($a_{\text{SiGe}}^{\parallel}$) lattice constants of strained $\text{Si}_{1-x}\text{Ge}_x$ deposited on Si (100) with Ge fractions (x) can be calculated from measured angles using the following equations:

$$a_{\text{SiGe}}(x) = \left(\frac{1-\nu}{1+\nu} \right) a_{\text{SiGe}}^{\perp}(x) + \frac{2\nu}{1+\nu} a_{\text{SiGe}}^{\parallel}(x) \quad (1)$$

$$a_{\text{SiGe}}(x) = 5.4309 + 0.200326x + 0.027274x^2 \quad (2)$$

where $a_{\text{SiGe}}(x)$ is the lattice constant of fully relaxed $\text{Si}_{1-x}\text{Ge}_x$ and ν is Poisson's ratio along the (001) direction. We adopted $\nu_{\text{Si}} = 0.278$ and $\nu_{\text{Ge}} = 0.271$. The nonlinear dependence of the $\text{Si}_{1-x}\text{Ge}_x$ unstrained lattice constant on the Ge composition (x) is given by Eq. (2) [18]. From Eqs. (1) and (2), the angle (θ_C) measured by MEIS between the incident beam and the scattered beam can be calculated by Eq. (3) :

$$\theta_C = 180 - \cos^{-1} \left(\frac{1}{\sqrt{1 + \left(\frac{\sqrt{2} a_{\text{SiGe}}^{\perp}(x)}{a_{\text{SiGe}}^{\parallel}(x)} \right)^2}} \right) \quad (3)$$

Therefore, the blocking dip shift suggests that the change in the lattice parameter of the oxidized $\text{Si}_{0.7}\text{Ge}_{0.3}$ along the (001) direction (i.e. shift to a higher scattering angle) illustrated an increase of the lattice parameter, while the change to a lower scattering angle decreased the vertical lattice distance. Thus, the increase of the Ge concentration in the Ge pile-up layer enhanced the compressive strain in the surface of the Ge pile-up layer, resulting in a positive shift of the blocking dip. However, the negative shift of the blocking dip could not be explained by an increase in Ge concentration when the strain in the Ge pile-up layer did not relax, because the compressive strain in the Ge pile-up layer rose as the Ge concentration increased. The negative shift of the blocking dip indicated that partial relaxation could occur at the layer beneath the surface of the Ge pile-up layer due to the enhanced strain in the Ge pile-up layer.

The shifts of the blocking dip in oxidized $\text{Si}_{0.7}\text{Ge}_{0.3}$ for 30 min and 120 min can be calculated from the Ge fraction in previous AES results [15] using Eqs. (1)–(3). The values of oxidized $\text{Si}_{0.7}\text{Ge}_{0.3}$ for 30 and 120 min were 0.22 and 0.26°, while the measured values were 0.24 and 0.15°, respectively. The maximum Ge concentration of $\text{Si}_{0.7}\text{Ge}_{0.3}$ oxidized for 120 min was higher than that for 30 min. Thus, the value of the maximum positive shift for 120 min was larger than for 30 min when strain relaxation did not occur. However, the value for the maximum positive shift and the minimum negative shift of $\text{Si}_{0.7}\text{Ge}_{0.3}$ oxidized for 120 min were smaller than that for 30 min (Figs. 3 and 4), indicating that the strains in the Ge pile-up layer started to relax after oxidation for 30 min. The critical thicknesses of $\text{Si}_{0.55}\text{Ge}_{0.45}$ and $\text{Si}_{0.45}\text{Ge}_{0.55}$ grown at 900 °C were approximately 5 nm and 4 nm, respectively [19]. The thickness of the Ge pile-up layer for $\text{Si}_{0.7}\text{Ge}_{0.3}$ oxidized for 120 min was thicker than the critical thickness for $\text{Si}_{0.45}\text{Ge}_{0.55}$. Unfortunately, it was difficult to obtain the relaxation thickness compared with the critical thickness, because Ge concentration is graded through the Ge pile-up layer; however, we evaluated the reason for relaxation by investigating the negative shift of blocking dipo.

The shift of the blocking dip to negative angles can result in two possible relaxation mechanisms, namely, plastic and elastic deformation. The negative shift region of the blocking dipo of $\text{Si}_{0.7}\text{Ge}_{0.3}$ oxidized for 30 min was located from 94 keV to 92 keV, with the shifts slowly increasing along the deeper depth compared with decreasing shift.

However, for the 120 min oxidation, the negative shift started at 93 keV and rapidly increased until 91 keV, which was after the minimum shift. When the remaining initial $\text{Si}_{0.7}\text{Ge}_{0.3}$ layers were fully relaxed, the angle of the blocking dip could not change with a variation of Ge concentration because a_{SiGe}^{\perp} can equal $a_{\text{SiGe}}^{\parallel}$, after which the number of shifts from the blocking dip of fully strained $\text{Si}_{0.7}\text{Ge}_{0.3}$ could be calculated from Eq. (3) as -0.28° . The minimum values of the negative shifts for $\text{Si}_{0.7}\text{Ge}_{0.3}$ oxidized for 30 min and 120 min were -0.15° and -0.21° , indicating that the remaining initial $\text{Si}_{0.7}\text{Ge}_{0.3}$ under the Ge pile-up layer was partially relaxed and that the rate of relaxation increased with oxidation time. If the relaxation had occurred by elastic deformation of the enhanced strain in the Ge pile-up layer, the negative shift for 120 min would have been similar or larger than that for 30 min, because the strain in the Ge pile-up layer for $\text{Si}_{0.7}\text{Ge}_{0.3}$ oxidized for 120 min was relaxed. Therefore, the relaxation of oxidized $\text{Si}_{0.7}\text{Ge}_{0.3}$ for 120 min was due to plastic deformation of the lattice structure.

The most probable relaxation process occurred through the plastic deformation process in spite of no defects in the pile-up layer (Fig. 1), which is very similar to the case of the formation of the threading dislocation. Moreover, the relaxation of the Ge pile-up layer appeared in the Ge pile-up layer, and the remaining initial $\text{Si}_{0.7}\text{Ge}_{0.3}$ layer appeared just beneath the Ge pile-up layer. The diffusion of Ge atoms to substitution sites in the lattice became difficult when the Ge concentration was high, because the presence of Si atoms switching with Ge atoms decreased with an increasing Ge concentration. The redistribution of Ge atoms can occur easily by switching at the top surface of the Ge pile-up layer because a high density of vacancy is generated by the diffusion of Si atoms to form oxides. On the other hand, the redistribution of Ge atoms caused by the incorporation of Ge atoms to interstitial sites has a relatively small probability of diffusion of Si. The incorporated Ge atoms at interstitial sites in the lattice structure can enhance the higher strain in the $\text{Si}_{1-x}\text{Ge}_x$ layer, illustrating that the relaxation of strain can occur in both the Ge pile-up layer and the $\text{Si}_{0.7}\text{Ge}_{0.3}$ layer just beneath the Ge pile-up layer.

4. Conclusion

In this study, the strain in the Ge pile-up layer on a $\text{Si}_{0.7}\text{Ge}_{0.3}$ film generated by selective oxidation was investigated with MEIS measurements. The strain in the top surface of the Ge pile-up layer was enhanced by oxidation and was affected by oxidation length. Partially relaxed layers were observed beneath the Ge pile-up layer, the presence of which could not have occurred without the generation of dislocations. Relaxation of the Ge pile-up layer affected the strain in the depth direction, and an oppositely oriented strain appeared under the pile-up layer. The partial relaxation was due to the increased strain in the Ge pile-up layer and the redistribution of Ge atoms by oxidation. The relaxation of the strain in oxidized $\text{Si}_{0.7}\text{Ge}_{0.3}$ increased with oxidation time. Through this work, we suggest a relaxation mechanism of $\text{Si}_{1-x}\text{Ge}_x$ by oxidation.

Acknowledgments

This work was supported by the IT R&D program of MKE/IITA [2008-F-023-01, Next generation future device fabricated by using nano junction] and "System IC 2010" project of the Korea Ministry of Commerce, Industry and Energy.

References

- [1] C.K. Maiti, L.K. Bera, S. Chattopadhyay, *Semicond. Sci. Technol.* 13 (1998) 1225.
- [2] D.K. Nayak, J.C.S. Woo, J.S. Park, K.L. Wang, K.P. Macwilliams, *IEEE Electron Dev. Lett.* 12 (1991) 154.
- [3] D.K. Nayak, K. Goto, A. Yutani, J. Murota, Y. Shiraki, *IEEE Electron Dev. Lett.* 43 (1996) 1709.
- [4] C.K. Maiti, L.K. Bera, S.S. Dey, D.K. Nayak, N.B. Chakrabarti, *Solid-State Electron.* 41 (1997) 1863.
- [5] K. Ismail, J.O. Chu, B.S. Meyerson, *Appl. Phys. Lett.* 64 (1994) 3124.

- [6] M.T. Currie, S.B. Samavedam, T.A. Langdo, C.W. Leitz, E.A. Fitzgerald, *Appl. Phys. Lett.* 72 (1998) 1718.
- [7] M. Arafa, P. Fay, K. Ismail, J.O. Chu, B.S. Meyerson, I. Adesida, *IEEE Electron Device Lett.* 17 (1996) 124.
- [8] S. Nakaharai, T. Tezuka, N. Sugiyama, Y. Noriyama, S. Takagi, *Appl. Phys. Lett.* 83 (2003) 3516.
- [9] T. Tezuka, N. Sugiyama, T. Mizuno, S. Takagi, *IEEE Trans. Electron Devices* 50 (2003) 1328.
- [10] F.K. LeGoues, R. Rosenberg, T. Nguyen, F. Himpfel, B.S. Meyerson, *J. Appl. Phys.* 65 (1989) 1724.
- [11] D. Nayak, K. Kamjoo, J.C.S. Woo, J.S. Park, K.L. Wang, *Appl. Phys. Lett.* 56 (1990) 66.
- [12] D.K. Nayak, K. Kamjoo, J.S. Park, J.C.S. Woo, K.L. Wang, *Appl. Phys. Lett.* 57 (1990) 369.
- [13] F.K. LeGoues, R. Rosenberg, B.S. Meyerson, *Appl. Phys. Lett.* 54 (1989) 644.
- [14] J.C. Lee, C.S. Chung, H.J. Kang, Y.P. Kim, H.K. Kim, D.W. Moon, *J. Vac. Sci. Technol. A* 13 (1995) 1325.
- [15] B.-G. Min, Y.H. Pae, K.S. Jun, D.-H. Ko, H. Kim, M.-H. Cho, T.-W. Lee, *J. Appl. Phys.* 100 (2006) 016102.
- [16] J.M. Hartmann, B. Gallas, J. Zhang, J.J. Harris, *Semicond. Sci. Technol.* 15 (2000) 370.
- [17] S. Nakashima, T. Mitani, M. Ninomiya, K. Matsumoto, *J. Appl. Phys.* 99 (2006) 053512.
- [18] J.P. Dismukes, L. Ekstrom, R.J. Paff, *J. Phys. Chem.* 68 (1964) 3021.
- [19] D.C. Houghton, *J. Appl. Phys.* 70 (1991) 2136.